

## Zirconia Effect on the Bioactivity and the Mechanical Properties of Calcium Magnesium Silicate Ceramics at (CaO+MgO)/SiO<sub>2</sub> Molar Ratio Close to Unity

Amira MM Amin<sup>1</sup>, Emad MM Ewais<sup>1\*</sup>, Yasser MZ Ahmed<sup>1</sup>, Eman A Ashor<sup>2</sup>, Ulrike Hess<sup>3</sup> and Kurosch Rezwan<sup>3</sup>

<sup>1</sup>Refractory and Ceramic Materials Division (RCMD), Advanced Materials Department, Central Metallurgical R and D Institute (CMRDI), P.O. Box 87, Helwan, 11421 Cairo, Egypt

<sup>2</sup>Chemical Engineering Department, Faculty of Engineering, El-Minia University, El-Minia, Egypt

<sup>3</sup>Advanced Ceramics, University of Bremen, Am Biologischen Garten 2, 28359 Bremen, Germany

### Abstract

New ceramic composites from calcia-magnesia-silica system at a molar ratio of (CaO-MgO)/SiO<sub>2</sub> closes to the unity and the addition of different amounts of zirconia (5 wt %, 15 wt % and 25 wt %) have been investigated. These systems powders were formed and fired at 1310 ± 20°C for 2 hr. Phase composition, microstructure, physical and mechanical properties of these composites were determined. The in-vitro bioactivities of these sintered composites were investigated by analysis of their ability for the formation of hydroxyapatite (HA) using SEM-EDS after their soaking in the simulated body fluid (SBF) for 7 days. The findings indicated that beginning of HA formation on the surface of all investigated composites. However, the composite containing 5 wt % ZrO<sub>2</sub> gave clear tendency toward the formation-ability of HA typical to cauliflower morphology. The mechanical properties of the promised bioactive composite in term of Vickers hardness and fracture toughness were ~3 Gpa and ~2 Mpa. m<sup>1/2</sup>, respectively. The ceramic composite containing 5 wt % ZrO<sub>2</sub> might be nominated to be implanted material because their property is quite similar to the properties of human cortical bone.

**Keywords:** Bioactivity; Calcia; Magnesia; Zirconia; SBF; Microstructure; Vickers hardness; Fracture toughness

### Introduction

As a result of good chemical stability and mechanical properties of zirconia ceramics, they have been used in ball heads of total hip replacement (THR) [1]. In addition, zirconia is considered as a bio-inert ceramics because when it implanted in living bone, it showed only a morphological fixation with surrounding tissues without producing any chemical or biological bonds. On the other hand, bioactive calcium magnesium silicate ceramics are able to bond to living bone via the formation of a bone like apatite layer on their surfaces [1,2]. Since bioactive calcium magnesium silicate ceramics have poor mechanical properties, they are used as coatings on tougher non-bioactive substrates such as zirconia and alumina ceramics or metal [3-9]. Therefore, to combine the favorable mechanical properties and bioactivity, bioinert zirconia is coated with bioactive materials (bioactive glasses and hydroxyapatite). However, there is also still shortcoming of coating materials for some targeted medical applications. Generally, the main requirements of the biomaterial, it must have high biological and mechanical properties. Concerning ZrO<sub>2</sub> ceramics, the essential requirement is the enhancement of their bioactivities, i.e., conversion of their non-bioactivities into bioactivities. In addition, mechanical properties of calcium magnesium silicate must be enhanced. As reported previously, this can be achieved through the coating of zirconia ceramics by bioactive materials (glass or hydroxyapatite) or biomimetic method. The latter, it can be conducted by different ways; 1-chemical treatment with different aqueous solution [10] 2- re-immersion method by more concentrated solutions (1.4 SBF, 1.5 SBF and 5 SBF) [11] and 3- presence of bioactive materials (e.g., bioactive glass or wollastonite beds) in the first time of immersion in SBF (first 7 days) followed by re-immersion in more concentrated solutions (1.4 SBF) for 14 days [12]. These scenarios especially no. 3 must be highlighted and motivate academicians to be considered. In the current study, new ceramic composites from the calcia magnesia silica system at (C+M)/S of ~1 with different additions of zirconia were investigated.

This study aims at developing of ceramic composites with promised bioactivity and enhanced mechanical properties.

### Materials and Experimental Procedure

#### Materials

Calcium carbonate as a source of calcia (C: CaO), magnesia (M: MgO) that are used in this study are chemically grade materials. They were supplied by Fisher chemical, UK, and LOBA Chemie for laboratory reagents and fine chemicals, India for CaCO<sub>3</sub> and MgO, respectively. Purity of MgO heavy extra powder was 99% and its particle size was <5 µm. While zirconia (Z: ZrO<sub>2</sub>) and quartz as a source of silica (S: SiO<sub>2</sub>) were provided by, SEPR, France and El-Nasr Company for Refractories and Ceramics, Sornaga, Egypt, respectively. The chemical analysis of zirconia and silica powders supported by analytical XRF (Model advanced axios Netherlands) is given in Table 1. The particle size of zirconia and silica is given in Table 2. The particle size distribution of zirconia and silica was measured using a laser light-scattering particle-size analyzer (Model LB500, Horiba, Tokyo).

\*Corresponding author: Emad M M Ewais, Refractory and Ceramic Materials Division (RCMD), Advanced Materials Department, Central Metallurgical R and D Institute (CMRDI), P.O. Box 87, Helwan, 11421 Cairo, Egypt, Tel: 201002395435; Fax: 20238621782; E-mail: [dr\\_ewais@hotmail.com](mailto:dr_ewais@hotmail.com)

Received December 19, 2015; Accepted January 08, 2016; Published January 19, 2016

**Citation:** Amin AMM, Ewais EMM, Ahmed YMZ, Ashor EA, Hess U, et al. (2016) Zirconia Effect on the Bioactivity and the Mechanical Properties of Calcium Magnesium Silicate Ceramics at (CaO+MgO)/SiO<sub>2</sub> Molar Ratio Close to Unity. Bioceram Dev Appl 6: 088. doi:10.4172/2090-5025.100088

**Copyright:** © 2015 Amin AMM, et al. This is an open-access article distributed under the terms of the Creative Commons Attribution License, which permits unrestricted use, distribution, and reproduction in any medium, provided the original author and source are credited.

	Chemical Composition, wt %	
	Silica	Zirconia
ZrO <sub>2</sub>	-	98.323
SiO <sub>2</sub>	97.93	0.746
Al <sub>2</sub> O <sub>3</sub>	0.85	0.303
Na <sub>2</sub> O	0.1	0.127
MgO	0.08	-
P <sub>2</sub> O <sub>5</sub>	-	0.063
SO <sub>3</sub>	-	-
K <sub>2</sub> O	0.1	-
CaO	0.84	0.156
TiO <sub>2</sub>	0.1	0.114
Fe <sub>2</sub> O <sub>3</sub>	-	0.117
F	-	-
Cl	-	0.05
L.O.I	-	-

Table 1: Chemical composition analysis of silica and zirconia as measured by XRF.

Material	Particle size, μm		
	d <sub>10</sub>	d <sub>50</sub>	d <sub>90</sub>
Silica	2.686	25.95	104.7
Zirconia	1.325	5.378	13.95

Table 2: Particle size distribution of silica and zirconia powders.

Mixture	Composition, Wt %			
	SiO <sub>2</sub>	CaCO <sub>3</sub>	MgO	ZrO <sub>2</sub>
A	44.78	40.16	15	0
B	42.54	38.152	14.25	5
C	38.063	34.136	12.75	15
D	33.584	30.12	11.25	25

Table 3: Compositions of A, B, C and D composites.

## Experimental procedure

Calcium magnesium silica mixtures of a molar ratio of 1.04 with different amounts of zirconia (5 wt %-25 wt. % with 10 wt. % intervals) were prepared as given in Table 3. The compositions containing 0 wt %, 5 wt %, 15 wt %, 25 wt % of ZrO<sub>2</sub> were termed as A, B, C and D, respectively. The mixtures were wet mixed with ethanol in a planetary mill for 45 min using a zirconia ball to produce a homogenous mixture. The mixtures were dried and ground to pass through a 0.1 mm sieve. The powders were uni-axially pressed (KPD-30A, Spain) at 60 MPa into a cylindrical shape of 2.3 cm diameter and 1cm length. The specimens were dried for 24 hr in oven at 110°C, and then fired at 1310 ± 20°C for 2 hr in a programmable electric furnace (HT 16/17, Nabertherm, Germany). The temperature of the specimens was raised from room temperature to the maximum firing temperature with constant rate of 4°C/min.

## Characterization

Phase composition and crystalline phases in sintered specimens were identified by advanced X-ray powder diffraction using Burker advanced X-ray diffractometer model D8 Kristalloflex (Ni-filtered Cu Kα radiation; λ=1.544 Å, Germany). In addition, the Crystallite sizes were calculated from the XRD pattern by applying Scherrer's equation. Microstructural features of the sintered specimens were characterized using a field emission scanning electron microscope (FESEM; QUANTA FEG250 Made in NL). The surfaces of the specimens

were examined using backscattered electron signals (BSE). Elemental analysis of each phase was also performed using the energy dispersive X-ray spectroscopy (EDX) equipped in the FESEM.

The apatite-formation ability of the obtained sintered specimens were evaluated by soaking in a simulated body fluid (SBF) solution at pH 7.45 and temperature of 36.5°C for 7 days. The SBF solution was prepared according to the procedure [13]. After soaking for 7 days, the specimens were filtrated, rinsed with water, dried at ambient conditions and characterized by SEM. Apparent porosity and bulk density of sintered specimens were determined by an Archimedes immersion technique using kerosene [14].

Vickers hardness (H<sub>v</sub>) and fracture toughness (K<sub>IC</sub>) of the obtained ceramic specimens were determined at room temperature on the polished surface considering an average of five indentations using a Vickers indentation method [15-19] with 20 kg load for 15 s. Vickers hardness was computed using the following relation:

$H_v = 0.0018544 (p/d^2)$  Where p is the indentation load (N), d is an average length of the two diagonals of the indentation, (mm) and H<sub>v</sub> is the Vickers hardness in the unit of (GPa). On the other hand, the fracture toughness was calculated through applying one of the following formulas based on the type of crack [20-22].

$$K_{IC} = 0.0515 p/c^{3/2} \quad \text{for Palmqvist shaped-crack}$$

$$K_{IC} = 0.0726 p/c^{3/2} \quad \text{for half-penny shaped-crack}$$

Where c is the crack length measured from the middle of the Vickers indentation (m), p is the indentation load (N) and K<sub>IC</sub> is the fracture toughness (MPa. m<sup>1/2</sup>).

## Results and Discussion

### Phase composition

The XRD patterns of the four composites mixtures A, B, C and D are shown in Figure 1. The pattern of the sintered specimen A shows that it is composed of diopside phase (CaMg(SiO<sub>3</sub>)<sub>2</sub> JCPDS 19-0239) with crystalite size of 131.2 nm as a major phase and akermanite phase (Ca<sub>3</sub>Mg(Si<sub>2</sub>O<sub>7</sub>)<sub>2</sub> JCPDS 76-0841) with crystalite size of 77.2 nm as a minor phase. It was obvious that, baddeleyite (ZrO<sub>2</sub> JCPDS 13-0307) emerges at the expense of the diopside and akermanite phases with addition of ZrO<sub>2</sub> from 5 wt % to 25 wt % (mixtures B, C and D). Interestingly, the

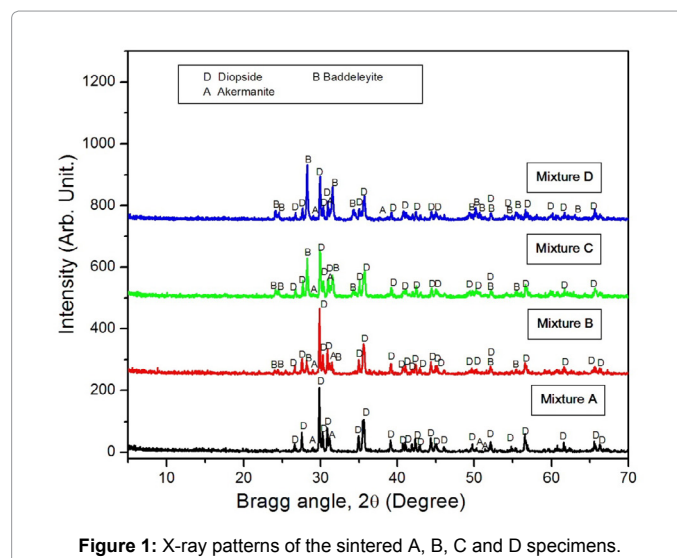


Figure 1: X-ray patterns of the sintered A, B, C and D specimens.

addition of zirconia didn't show any reaction with the other constituents and remains in a monoclinic polymorph (baddeleyite). It seems that MgO, CaO, SiO<sub>2</sub> in this batch were stoichiometrically equivalent to diopside and akermanite. Therefore, no sufficient calcia or magnesia is present to react with zirconia. This explains the remaining of zirconia in the monoclinic form. It worth noting that the mixture containing calcia-silica-magnesia with a molar ratio of (C+M)/S without zirconia addition was sintered at 1310°C, while the sintering temperature of the other mixtures containing zirconia were raised to 1330°C. This is due to the addition of baddeleyite phase, which has a high melting point.

### Microstructure

FESEM micrographs of the sintered specimens containing various ZrO<sub>2</sub> content are illustrated in Figures 2a-2h. As seen in Figures 2a, 2c, 2e and 2g, the phases and pores are uniformly distributed and the level of pores seems to be very low (3%). Generally, there are two phases; one of them is light white color and the other is dark gray colors as shown in Figures 2b, 2d, 2f, 2h. Their EDX analysis indicates that the light white grains are zirconium oxide with two morphologies; one is a small rounded shape and the other is a large with irregular shape. The dark grey interface with sharp edges is diopside.

### Physico-mechanical properties

The densification parameters in terms of bulk densities, apparent porosity and linear shrinkage of sintered specimens (A-D) are given in Table 4. It can be seen that there is a slight change of the apparent porosity and bulk density with increasing the addition of zirconia. Bulk density of the investigated specimens increased from 2.95 g/cm<sup>3</sup> to 3.34 g/cm<sup>3</sup>. The recorded change of the bulk density of the composites

Mixture	Bulk density, g/cm <sup>3</sup>	Apparent porosity, %	Linear shrinkage, %
A	2.95	4.5	12.82
B	3.07	3.2	15.11
C	3.17	3.05	19.69
D	3.34	3.77	21.08

Table 4: Physical properties of the sintered A, B, C and D specimens.

Mixture	Hardness, GPa
A	3.5
B	3.18
C	2.57
D	2.17

Table 5: Vickers hardness of the sintered A, B, C, and D specimens.

containing 0 wt %-25 wt % ZrO<sub>2</sub> can be attributed to; 1- the decrease of the porosity from 4.5% to 3.77% as results of the increase of the linear shrinkage from 12.82% to 21.08%, and 2- the increase of high density zirconia phase (5.75 g/cm<sup>3</sup>). The mechanical parameters in terms of Vickers hardness and fracture toughness are recorded in Tables 5 and 6. The hardness of the investigated composites significantly decreased from 3.5 GPa to 2.17 GPa with the increase of ZrO<sub>2</sub> content from 0 wt % to 25 wt %. The remarkable decrease in the hardness of these composites may be attributed to the decrease of the diopside phase of hardness value ranged from 4.9 GPa - 6.1 GPa [23]. The investigated composites, whether they have zirconia or have not, show palmqvist crack which reflects high toughness values (K<sub>IC</sub>). By applying the indentation fracture equation of the palmqvist crack to calculate the fracture toughness (K<sub>IC</sub>) values, it was found that, the fracture toughness (K<sub>IC</sub>) values increased from 2.40 K<sub>IC</sub> to 2.99 K<sub>IC</sub>, MPa.m<sup>1/2</sup> with the increase of ZrO<sub>2</sub> addition up to 25 wt %. This may be understood through the presence of high fracture toughness zirconia phase in monoclinic form (m-ZrO<sub>2</sub>), which is characterized by its martensitic transformation from monoclinic to tetragonal zirconia (m-ZrO<sub>2</sub> ↔ t-ZrO<sub>2</sub>) under cooling from sintering temperature to room temperature. Such kind of transformation arrests the crack propagation and in turn improves the fracture toughness (K<sub>IC</sub>) [24]. Table 7 gives the mechanical, physical and biological properties of all composites (A-D) and the most bioceramic materials which reported in the literature and cortical bone [25-30]. These reported values of the physical and mechanical tested values are compatible with the properties of the cortical bone.

### In-vitro bioactivity of the composites

Figures 3a-3d, shows the SEM micrographs and EDX of the investigated ceramic composites made of calcia, magnesia and silica mixture of a molar (C+M)/S ratio of 1.04 with various amounts of ZrO<sub>2</sub> content after soaking in simulated body fluid (SBF) for 7 days. It was found that, the surface of the composite B was completely covered the apatite. The morphology of this apatite is very unique and typically cauliflower with typical drying cracks, see Figure 3b. In contrast, the nucleation of hydroxyapatite was started to be appeared on the surface of the ceramic composites containing 0 wt %, 15 wt % and 25 wt % ZrO<sub>2</sub>, see Figures 3a, 3c and 3d. The beginning of apatite formation during 7 days on the surface of the sintered specimen (without zirconia) can be rationalized based on the akermanite phase because akermanite phase has good apatite mineralization and moderate dissolution and induces bone-like apatite formation after 5 days [31]. In another study, it was pointed that pure akermanite powders synthesized by sol-gel method and calcination at 1300°C induce hydroxylapatite formation on their surface after 10 days [32]. Herein, the addition of ZrO<sub>2</sub> greatly

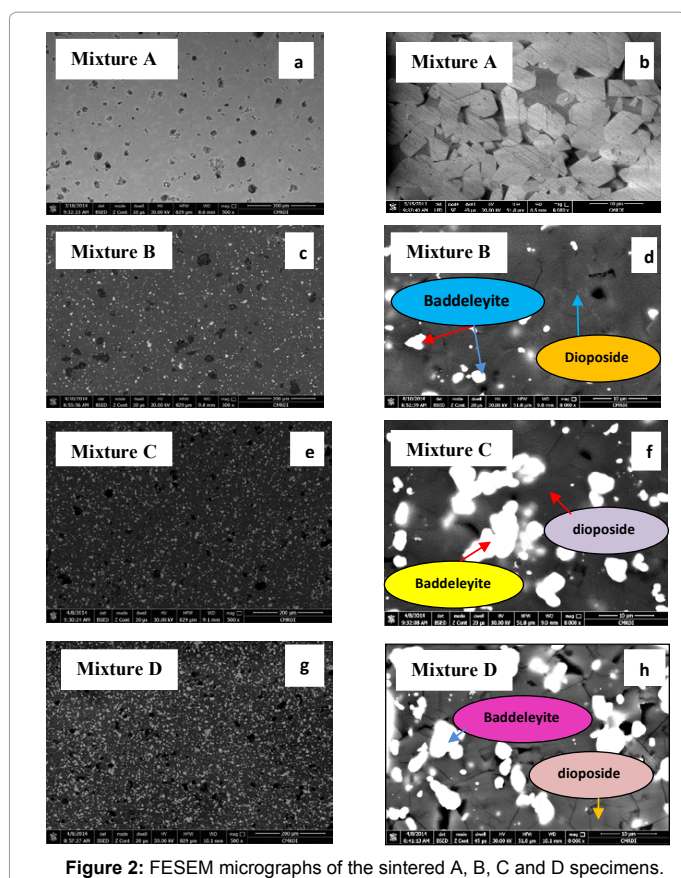


Figure 2: FESEM micrographs of the sintered A, B, C and D specimens.

Mixture	Cav (mm)	a (mm)	C/a	Crack type	K <sub>IC</sub> , MPa.m <sup>1/2</sup>
A	0.268	0.16	1.675	palmqvist	2.4
B	0.281	0.175	1.6	palmqvist	2.45
C	0.33	0.225	1.47	palmqvist	2.5
D	0.225	0.125	1.8	palmqvist	2.99

Table 6: Crack pattern resulted from indentation fracture at 20 kg of the sintered A, B, C and D specimens.

Material	Mixture (A)	Mixture (B)	Mixture (C)	Mixture (D)	Bredigite	Wollastonite Coating	HA Coating	Akermanite	HA	γ-dicalciumsilicate	Diopside	Cortical bone
Hardness	3.5	3.18	2.57	2.17	-----	2.5	1.2	-----	6	3.62	-----	1-2.3
Fracture Toughness	2.4	2.45	2.5	2.99	1.57	-----	-----	1.83	0.75-1	1.48	3.2	6-Feb
Density	2.95	3.07	3.17	3.34	-----	2.6	3.1	-----	3.16	-----	3.2	1.6-2.1
Porosity	4.5	3.2	3.05	3.77	-----	5.3	7	-----	-----	-----	-----	-----
Bioactivity	moderate	fast	moderate	moderate	fast	moderate	moderate	moderate	fast	fast	slow	-----

Table 7: The comparison of the properties of sintered specimens, the most bioceramic materials reported in the literature and cortical bone.

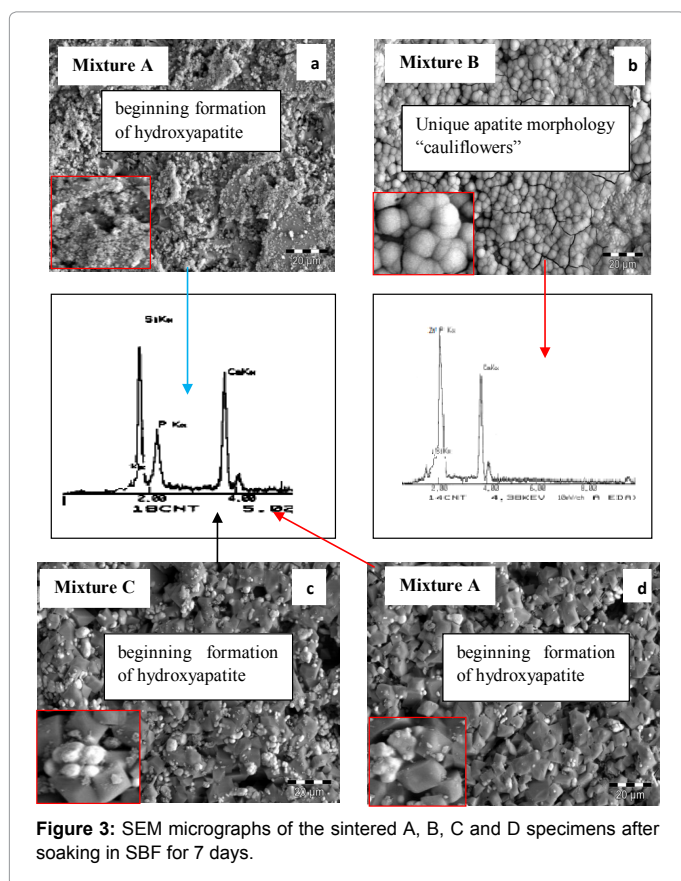


Figure 3: SEM micrographs of the sintered A, B, C and D specimens after soaking in SBF for 7 days.

enhances the bioactivity in particular with 5 wt % as shown in Figure 3a. Interestingly, the bone-like apatite formation extremely increased with increasing zirconia content up to 5 wt %. This result was not expected because the increase of zirconia content is accompanied by decreasing the content of the bioactive phase (akermanite). With the continuing increase of zirconia content up to 25 wt %, bone-like apatite formation was gradually decreased again. Bone-like apatite formation (bioactivity) greatly depends on phase composition and physical properties of the materials. Since the physical properties of all specimens are quite similar, the tendency of the specimens to form bone-like apatite based this factor must be excluded. The difference between specimens

compositions are the content of zirconia at the expense of the phases developed during sintering such as akermanite and, see XRD patterns of the specimens Figure 1. In the view of the bioactivity, akermanite and its content were considered the effective element. Also, zirconia content (baddeleyite) and its reflection on the bioactivity of akermanite and vice versa were taken into consideration to understand the obtained data. The formation of layer bone-like apatite on the surface of the specimens containing 5 wt % zirconia placed in SBF can be explained based on the reported data. As previously investigated by Wu depletion of Ca, Mg and Si ions from akermanite phase into SBF starts to occur in the early stage (i.e., after one day) and their concentration increases with time. This process is accompanied by the increase of pH as results of ion exchange of Ca cations in the akermanite ceramics with H cations in SBF [31]. Consequently, a hydrated silica layer on the surface of the akermanite based ceramics and favorable sites for phosphate nucleation are formed. Accordingly, amorphous calcium phosphate with subsequent formation of bone-like apatite by incorporating OH anions from SBF. This mechanism is favorable with our results but the content of bone-like apatite seems to be proportional to the content of akermanite phase. Another possible reaction mechanism is expected to be occurred and responsible about the formation of layer bone-like apatite. Along with the little increase of the pH, hydroxylated zirconia surface (Zr-OH) is converted into negatively charged Zr-O bond. This in turns attracts Ca cations from SBF into the interface between the specimens and SBF then start to induce bone-like apatite nucleation in a similar manner as Si-OH [10,33]. In this context, it can be said that the amount of the akermanite phase in the specimen B is sufficient to give a reasonable concentration of Ca cations through ion exchange and increasing pH. This amount allows for the formation of bone-like apatite through ion exchange of Ca<sup>2+</sup> ion from the depleted akermanite into the SBF solution with surface negatively charged surface with functional groups (≡ Si-O<sup>-</sup> and Zr-O<sup>-</sup>). With the increase of zirconia content to from 15 wt % to 25 wt % at the expense of akermanite phase, the depleted amount of Ca<sup>2+</sup> cations seems to be not sufficient to increase the pH and in turn the activation of the zirconia surface seems to be difficult, therefore, the role of zirconia to induce bone-like apatite is neglected and the formation of the apatite mainly depends on the amount of the akermanite.

## Conclusion

Systematic mixtures based calcia-magnesia-silica with a molar ratio of 1.04 with different amounts of ZrO<sub>2</sub> (5 wt %, 15 wt %, and 25 wt %) were investigated. The results proved that developed ceramic

composite B made of a mixture from calcia, magnesia and silica with a (C+M)/S molar ratio and 5 wt % ZrO<sub>2</sub> good biological properties. Its physico-mechanical properties are similar to those of human cortical bone, see Table 7 Therefore, it might be a candidate material for bone implant.

#### References

- Hulbert SF (1993) The use of alumina and zirconia in surgical implants: in an introduction to bioceramics. World Scientific, Singapore PP.
- Kokubo T (1991) Recent progress in glass-based materials for biomedical applications. *J Ceram Soc Jpn* 99: 965-973.
- Liu X, Ding C, Chu PK (2004) Mechanism of apatite formation on wollastonite coatings in simulated body fluids. *Biomaterials* 25: 1755-1761.
- Ferraries M, Verne HE, Appendino P, Moisescu C, et al. (2000) Coatings on zirconia for medical applications. *Biomaterials* 21: 765-773.
- Bosetti M, Verne E, Ferraris M, Ravaglioli A, Cannas M (2001) In vitro characterisation of zirconia coated by bioactive glass. *Biomaterials* 22: 987-994.
- Gua YW, Yapb AUJ, Cheanga P, Khor KA (2005) Effects of incorporation of HA/ZrO<sub>2</sub> into glass ionomer cement (GIC). *Biomaterials* 26: 713-720.
- Kim HW, Lee SY, Bae CJ, Noh YJ, Kim HE (2003) Porous ZrO<sub>2</sub> bone scaffold coated with hydroxyapatite with flourapatite intermediate layer. *Biomaterials* 24: 3277-3284.
- Stanc V, Aldini NN, Fini M, Giavaresi G, et al. (2002) Osteointegration of bioactive glass -coated zirconia in healthy bone: an in vivo evaluation. *Biomaterials* 23: 3833-3841.
- Liu XY, Ding CX (2003) Bioactivity of plasma sprayed wollastonite/ZrO<sub>2</sub> composite coating. *Surf Coat Technol* 172: 270-278.
- Uchida M, Kim H-M, Koubo T, Nawa M, et al. (2002) Apatite forming ability of a zirconia alumina nano-composite induced by chemical treatment. *J Biomed Mater Res* 60: 277-282.
- Cortes DA, Nogiwa AA, Almanza JM, Ortega S (2005) Biomimetic apatite coating on Mg-PSZ/Al<sub>2</sub>O<sub>3</sub> composites Effect of the immersion method. *Materials Letters* 59: 1352-1355.
- Nogiwa AA, Cortes DA (2006) Bone-like apatite coating on Mg-PSZ/Al<sub>2</sub>O<sub>3</sub> composites using bioactive systems. *J Mater Sci Mater Med* 17: 1139-1144.
- Kokubo T, Takadama H (2006) How Useful is SBF in Predicting in Vivo Bone Bioactivity? *Biomaterials* 27: 2907-2915.
- ASTM C830-00 (2011) Standard Test Methods for Apparent Porosity, Liquid Absorption, Apparent Specific Gravity, and Bulk Density of Refractory Shapes by Vacuum Pressure.
- ASTM C1327-03 (2006) Test Method for Vickers indentation hardness of advanced ceramics. Annual Book of ASTM Standards ASTM West Conshohocken PA.
- Sergeje F, Antonov M (2006) Comparative Study on Indentation Fracture Toughness Measurements of Cemented Carbides. *Proc Estonian Acad Sci Eng* 12: 388-398.
- Bamzai KK, Kotru PN, Wanklyn BM (1998) Investigations on indentation induced hardness and fracture mechanism in flux grown DyAlO<sub>3</sub> crystals. *Appl Surf Sci* 133: 195-204.
- Yount HJ (2006) Hardness and fracture toughness of heat treated advanced ceramic materials for use as fuel coating and inert matrix materials in advanced reactors. University of Wisconsin Madison.
- Lawn HR, Fuller E R (1975) Equilibrium penny-like cracks in indentation fracture. *J Mater Sci* 10: 2016-2024.
- Keryvin V, Hoang VH, Shen J (2009) Hardness, toughness, brittleness and cracking systems in an iron-based bulk metallic glass by indentation. *Intermetallics* 17: 211-217.
- Curkovic L, Rede V, Grilec K, Mulabdic A (2007) Hardness and Fracture Toughness of Alumina Ceramics.
- Dietz M, Tietz HD (1990) Characterization of engineering ceramics by indentation methods. *J Mater Sci* 25: 3731-3738.
- Dornera D, Stockherta B (2004) Plastic Flow Strength of Jadeite and Diopside Investigated by Microindentation Hardness Tests. *Tectonophysics* 379: 227-238.
- Basu B (2005) Toughening of yttria-stabilised tetragonal zirconia ceramics. *Int Mater Rev* 50: 239-256.
- Li P, Zhang F (1990) The electrochemistry of a glass surface and its application to bioactive glass in solution. *J Non-Cryst Solids* 8: 112-119.
- Valet-Regi V, Salinas AJ, Roman J, Gil M (1999) Effect of magnesium content on the in vitro bioactivity of CaO-MgO-SiO<sub>2</sub>-P<sub>2</sub>O<sub>5</sub> sol-gel glasses. *J Mater Chem* 9: 515-518.
- Hench LL (1998) *Bioceramics*. *J Am Ceram Soc* 81: 1705-17028.
- Ravaglioli A, Krajewski A (1992) *Bioceramics-materials, Properties and applications*. London Chapman and Hall.
- Shi JL (1999) Thermodynamics and densification kinetics in solid-state sintering of ceramics. *J Mater Res* 14: 1398-1408.
- Rice RW (1996) Grain size and porosity dependence of ceramic fracture energy and toughness at 22°C. *J Mater Sci* 31: 1969-1983.
- Wu C, Chang J (2013) A review of bioactive silicate ceramics. *Biomed Mater* 8: 1-13.
- Wu CT, Chang J (2004) Synthesis and apatite-formation ability of akermanite. *Mater Lett* 58: 2415-2417.
- Uchida M, Kim HM, Kokubo T (2001) Bonelike apatite formation induced on zirconia gel in a simulated body fluid and its modified solutions. *J Am Ceram Soc* 84: 2041-2044.